Neuroscience 128 (2004) 871–887

TONOTOPIC AND HETEROTOPIC PROJECTION SYSTEMS IN PHYSIOLOGICALLY DEFINED AUDITORY CORTEX

C. C. LEE,[a]* C. E. SCHREINER,[b] K. IMAIZUMI[b] AND J. A. WINER[a]

[a]*Division of Neurobiology, Department of Molecular and Cell Biology, Room 285 Life Sciences Addition, University of California at Berkeley, Berkeley, CA 94720-3200, USA*

[b]*Coleman Memorial Laboratory, W. M. Keck Center for Integrative Neuroscience, University of California at San Francisco, San Francisco, CA 94143-0732, USA*

Abstract—Combined physiological and connectional studies show significant non-topographic extrinsic projections to frequency-specific domains in the cat auditory cortex. These frequency-mismatched loci in the thalamus, ipsilateral cortex, and commissural system complement the predicted topographic and tonotopic projections. Two tonotopic areas, the primary auditory cortex (AI) and the anterior auditory field (AAF), were electrophysiologically characterized by their frequency organization. Next, either cholera toxin β subunit or cholera toxin β subunit gold conjugate was injected into frequency-matched locations in each area to reveal the projection pattern from the thalamus and cortex. Most retrograde labeling was found at tonotopically appropriate locations within a 1 mm-wide strip in the thalamus and a 2–3 mm-wide expanse of cortex (approximately 85%). However, approximately 13–30% of the neurons originated from frequency-mismatched locations far from their predicted positions in thalamic nuclei and cortical areas, respectively. We propose that these heterotopic projections satisfy at least three criteria that may be necessary to support the magnitude and character of plastic changes in physiological studies. First, they are found in the thalamus, ipsilateral and commissural cortex; since this reorganization could arise from any of these routes and may involve each, such projections ought to occur in them. Second, they originate from nuclei and areas with or without tonotopy; it is likely that plasticity is not exclusively shaped by spectral influences and not limited to cochleotopic regions. Finally, the projections are appropriate in magnitude and sign to plausibly support such rearrangements; given the rapidity of some aspects of plastic changes, they should be mediated by substantial existing connections. Alternative roles for these heterotopic projections are also considered.

Key words: AI, AAF, thalamocortical projections, corticocortical projections, commissural system.

*Corresponding author. Tel: +1-510-642-9637; fax: +1-510-643-6791.
E-mail address: chazwell@uclink4.berkeley.edu. (C. C. Lee).

Abbreviations: AAF, anterior auditory field; ABC, avidin–biotin–peroxidase reaction; AI, primary auditory cortex; AII, secondary auditory cortical area; CF, characteristic frequency; CTβ, cholera toxin β subunit; CTβG, cholera toxin β subunit, gold-conjugated; EPD, posterior ectosylvian gyrus, dorsal part; EPI, posterior ectosylvian gyrus, intermediate part; PBS, phosphate-buffered saline.

The finding of rapid, massive, specific, and stable reorganization of auditory cortical sensory maps with behavioral training in primates (Recanzone et al., 1993) or concurrent sound stimulation and physiological activation of the nucleus basalis in rodents (Kilgard and Merzenich, 1998) represents a conceptual challenge to static theories of neuroanatomical connectivity. Before such experiments, the representation of characteristic frequency could be viewed as inflexible (Kaas, 1997; Weinberg, 1997). In particular, the speed and precision of reorganization across the frequency domain support the view that emergent representations contingent on widespread structural reorganization or sprouting are unlikely to subserve these global changes. On the other hand, there is no known latent, but otherwise masked, anatomical substrate that could credibly underlie such reorganizations, which extend from single neurons to substantial segments of the frequency domain (Weinberger, 1998; Galvan and Weinberger, 2002). In search of such a substrate, we have reexamined the principal extrinsic afferent connections of the auditory forebrain in physiologically mapped animals across the frequency domain. Our strategy entailed a qualitative and quantitative comparison of the patterns of thalamocortical, commissural, and corticocortical connections using sensitive retrograde tracers. By injecting different, and equally sensitive, tracers at matching tonotopic representations in two areas in a single hemisphere, we could determine how those presumptively corresponding loci were represented in the thalamus and ipsilateral and contralateral cortices (Lee et al., 2004). A finding of strict point-to-point connectivity—as predicted in certain models of thalamocortical relations (Brandner and Redies, 1990)—might support the notion that the widespread and non-topographic projections of nucleus basalis to cortex could be the critical element in eliciting experience-dependent reorganization.

Alternative hypotheses were also amenable to investigation in our model system. One possibility is that some qualitative or quantitative difference in the nature or strength of thalamic or cortical projections (Calford, 2002) might offer credible clues as to which latent connections might be dominant, or if the different systems have equal roles (Winer and Larue, 1987). A second alternative is that the areas chosen for our study—two tonotopic subdivisions of auditory cortexm, AI (primary auditory cortex) and AAF (anterior auditory field)—might have different or unique patterns of input that could offer clues about their capacity for rapid reorganization. A final hypothesis not tested directly here suggests a role for branched projections from frequency mismatched loci. Thus, if highly branched afferent axons form a prominent part of any of

0306-4522/04$30.00+0.00
doi:10.1016/j.neuroscience.2004.06.062

the projection systems, much as they do in other modalities (Bullier et al., 1984; Humphrey et al., 1985a; Kennedy and Bullier, 1985), their experience-dependent emergence (Wall, 1988) or "unmasking" (Jacobs and Donoghue, 1991; Schieber, 2001) could contribute to this reorganization and to long-term changes in frequency maps (Rajan et al., 1993). We report here the existence of spatially mismatched projections from multiple sources within each field; these connectional substrates appear sufficiently robust to serve as a credible candidate for inducing global experience-dependent plasticity.

EXPERIMENTAL PROCEDURES

Subjects and anesthesia

The right auditory cortex was studied in three female and one male, adult (>9 mos. old) cats. Our procedure followed protocols approved by the Institutional Animal Care and Use Committee of the University of California at San Francisco and the National Institutes of Health guidelines (NIH Publications No. 80–23 revised 1996) to minimize number and suffering of animals. After sedation with ketamine (22 mg/kg, i.m.) and acepromazine (0.11 mg/kg, i.m.), anesthesia was induced with sodium pentobarbital (15–30 mg/kg, i.v.) and a tracheotomy performed. The head was fixed in place while allowing free access to the ears. After retraction of the soft tissues a craniotomy was made above AI and AAF and the cortex was covered with mineral oil to prevent desiccation. For the duration of the experimental procedure an infusion of ketamine (1–3 mg/kg/h), diazepam (0.5–2 mg/kg/h), and lactated Ringer's solution (1–3 ml/kg/h) was maintained; one case received sodium pentobarbital and lactated Ringer's solution. Fluids were delivered continuously and body temperature was stabilized at approximately 37 °C with a water pad under positive control. Cardiac output and respiration were monitored continuously.

Physiological mapping

For the initial 24 h, characteristic frequencies (CFs) were mapped in AI and AAF at a high density to demarcate isofrequency contours and establish areal borders. The CF is the frequency at which a response was elicited by the lowest sound pressure level. Tungsten microelectrodes (0.5–2.5 MOhm) coated with Parylene recorded single- and multi-unit responses in the main thalamic recipient zone, layers IIIb and IV, at depths of 700–1100 μm (Winer, 1984; Huang and Winer, 2000). Microprocessor-generated (TMS32010, 16-bit D-A converter at 120 kHz) tone bursts (3-ms linear rise/fall; 50-ms duration; 400- to 700-ms interstimulus interval) were delivered through a STAX-54 headphone tube (Sokolich; U.S. Patent 4251686; 1981) inserted into the left external meatus. Unit responses from 675 pseudorandom tone bursts elicited at three to five octaves and across a 70 dB range were used to determine the excitatory frequency response area, from which the CF was derived. Subsequent analysis used MATLAB (MathWorks, Natick, MA, USA). Tonotopic maps were represented graphically by the Voronoi-Dirichlet tessellation (DELDIR, Statlib; Carnegie Mellon University, Pittsburgh, PA, USA), where polygon borders are defined at the centers between adjacent recording sites (Kilgard and Merzenich, 1998; Read et al., 2001).

Tract tracing

After the first day of mapping, either of two retrograde tracers—cholera toxin β subunit (CTβ) or CTβ/gold (CTβG; List Biological Laboratories, Campbell, CA, USA)—was injected at corresponding AI and AAF isofrequency loci. Locations of tracer injections were recorded on the physiological maps for later alignment. Glass pipettes (20–30 μm tip diameter) were filled with mineral oil in their shaft and tracer in the tip; these were advanced successively to 500, 1000, and 1500 μm below the pia, and a deposit was made at each depth. Using a nanoliter injector (World Precision Instruments, Sarasota, FL, USA) 55.2 nl of tracer was delivered at 4.6 nl/15 s to saturate this expanse. Two minutes between deposits allowed for tracer equilibration before pipette withdrawal. For the next 48–52 h, physiological recordings continued during tracer transport. Animals received a lethal dose of sodium pentobarbital and were perfused intracardially with phosphate-buffered saline (PBS; 0.01 M), then with 4% paraformaldehyde in 0.01 M PBS. After dissection the tissue was cryoprotected in 30% sucrose/4% paraformaldehyde in 0.01 M PBS for 3 days.

Histological processing

Coronal, 60 μm-thick frozen sections were cut and a 1:6 series was processed for each tracer. For CTβG, tissue was rinsed in 50% EtOH, washed in ddH_2O, silver-intensified for 3 h (Kierkegaard and Perry Laboratories, Gaithersburg, MD, USA), then washed in 1% sodium thiosulfate and rinsed in 0.01 M PBS. The CTβ sections were blocked for 1 h in 5% normal rabbit serum/0.3% Triton X-100, incubated overnight in goat anti-CTβ primary antibody (1:7500 dilution/0.01 M PBS; List Biological Laboratories), and intensified with the goat Vectastain avidin–biotin–peroxidase (ABC) kit (Vector Laboratories, Burlingame, CA, USA) using diaminobenzidine as the chromogen. Tissue was mounted onto gelatin-coated slides, cleared, and coverslipped.

Adjacent series of sections were prepared to document thalamic subdivisions and cortical areas with the Nissl stain or the SMI-32 antibody, which recognizes neurofilaments in pyramidal neurons (Campbell and Morrison, 1989) and demarcates AI. SMI-32 immunostaining began with blocking in normal horse serum/0.3% Triton X-100 (5%; 1 h), incubation with the SMI-32 antibody (1:2000 dilution in 0.01 M PBS; overnight; Sternberger Monoclonal Inc., Baltimore, MD, USA), then processing with a mouse Vectastain ABC kit (Vector Laboratories) and a heavy-metal-intensified DAB chromogen (Adams, 1981). Sections were mounted, cleared, and coverslipped as was the retrogradely labeled tissue. For the medial geniculate and posterior thalamus, a library of cell- and fiber-stained material was available, as well as various immunocytochemical preparations useful in documenting architectonic subdivisions (Huang et al., 1999). Thalamic and cortical subdivisions were drawn without knowledge of the labeling patterns.

Data analysis

The distribution of retrogradely labeled neurons was plotted with a microscope equipped with a motorized stage, through a proprietary imaging system superimposed on the microscope field (Lucivid), and stored on a computer equipped with the Neurolucida plotting and analysis software (MicroBrightField, Colchester, VT, USA). Retrogradely labeled neurons were plotted at 200× so that even faintly labeled neurons were included; both bright- and dark-field illumination were used as necessary. Plots were imported to Canvas 8 (Deneba Software Inc., Miami, FL, USA) and aligned with scanned 15× images of thalamic and cortical architectonic boundaries made independently from Nissl and immunocytochemical preparations. The distribution of labeled cortical neurons was projected onto two- and three-dimensional solids using the appropriate module in the Neuroexplorer analysis software (MicroBrightField). The three-dimensional model was imported to Canvas and aligned with surface landmarks from scale photographs of the brain in all planes to establish the surface lateral views of cortical labeling. The deposits and the lateral view of the cortex were reconstructed using photographs taken during recording and post-fixation photos of the brain before processing. These

recording site map photographs and the post-fixation photos were then aligned with the histological results, during which shrinkage was calculated and allowance was made for any distortion introduced during mounting. The resulting representation of the deposit sites, the mapping sites, and the loci of transport were thus reconciled with each other. Overlap of tracer deposits with the physiological recording sites was used to determine the frequencies encompassed by the injections. Counts of labeled neurons and quantitative measures used Neuroexplorer software.

Heterotopic labeling was defined as follows. In the ipsi- and contralateral tonotopic fields, a vertical line was drawn through the center of the heaviest focus of labeling. On either side of this line, a 1 mm zone was drawn, within which the labeling was classified as homotopic, that is, as within the isofrequency domain corre-

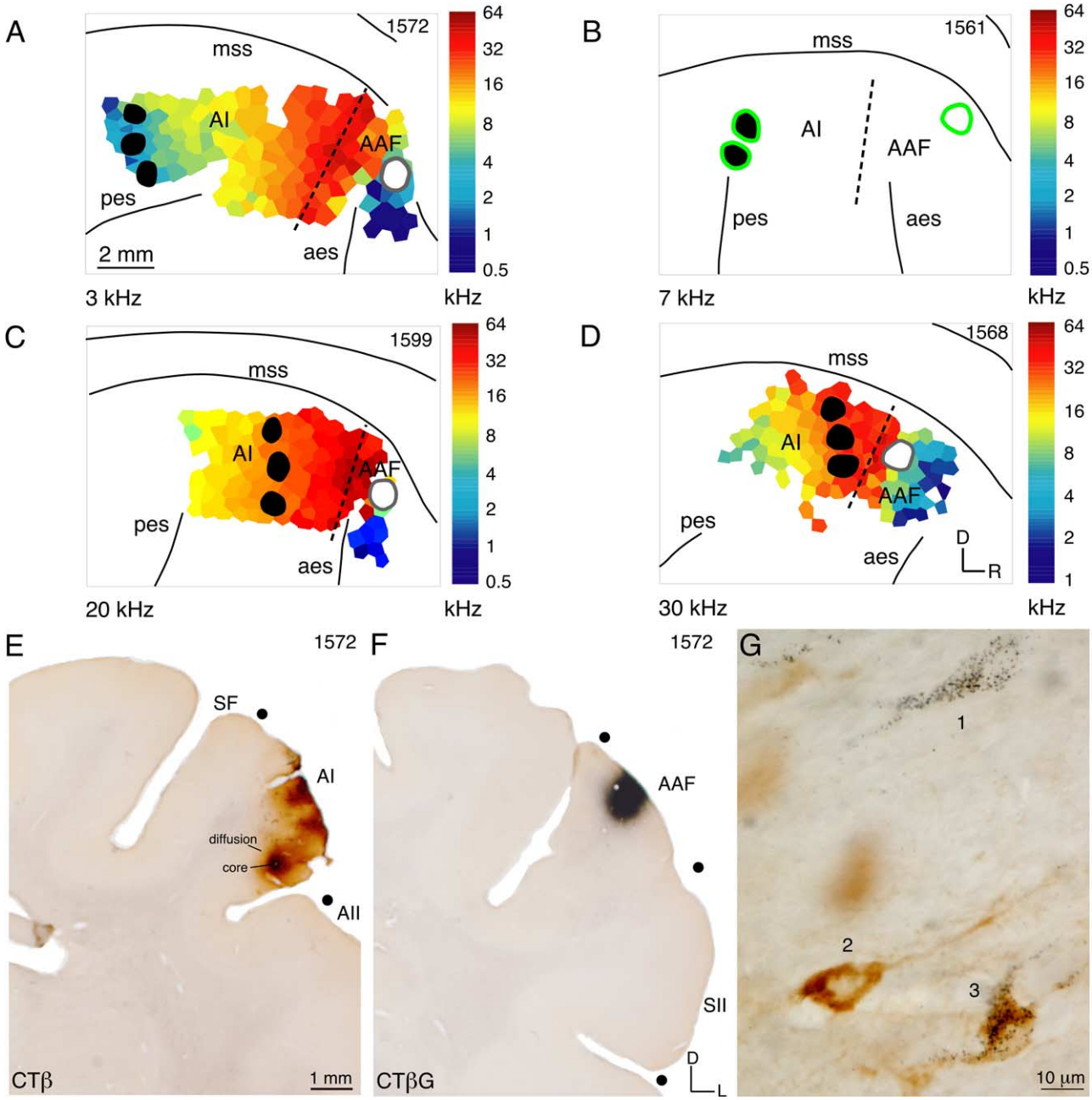

Fig. 1. Voronoi-Dirichlet tessellations illustrating the distribution of CF in four experiments projected onto a lateral view of the hemisphere (cf. Fig. 8A, right hemisphere). Each polygon represents the CF from one recording penetration. A dashed line indicates the border between areas. In the 7 kHz case (B), there were an insufficient number of recording penetrations to generate a detailed map. The CTβ injection sites (black ovals) and CTβG injection sites (white ovals) in AI and the AAF, respectively, are restricted to one octave representation. Injections at (A) 3 kHz, (B) 7 kHz, (C) 20 kHz, and (D) 30 kHz loci in both areas are confined to an isofrequency contour. Since the CF contours in AI and AAF differ in size, three deposits were usually made in the former, and one in the latter. Injection sites in the 3 kHz experiment are illustrated for the AI (E), and AAF (F) injections, with an estimate of their core (the presumptive effective deposit site) and diffusion, respectively. (G) Neurons labeled by CTβG (1), CTβ (2), or both (3) are readily distinguished from one another.

sponding to the deposit site. Labeling outside the zone is classified as heterotopic. For labeling in the injected area, this 1 mm zone extended from the perimeter of the deposits' diffusion, resulting in a 3 mm wide strip. This is a generous estimate of the actual dispersion of the injection since CTβ/CTβG have only limited diffusion and are not incorporated readily by fibers of passage (Llewellyn-Smith et al., 1990; Luppi et al., 1990; Ruigrok et al., 1995). In the thalamus, the homotopic boundary was set at 500 μm on each side of the center of labeling. The homotopic labeling was thus confined to the specified domains that were then

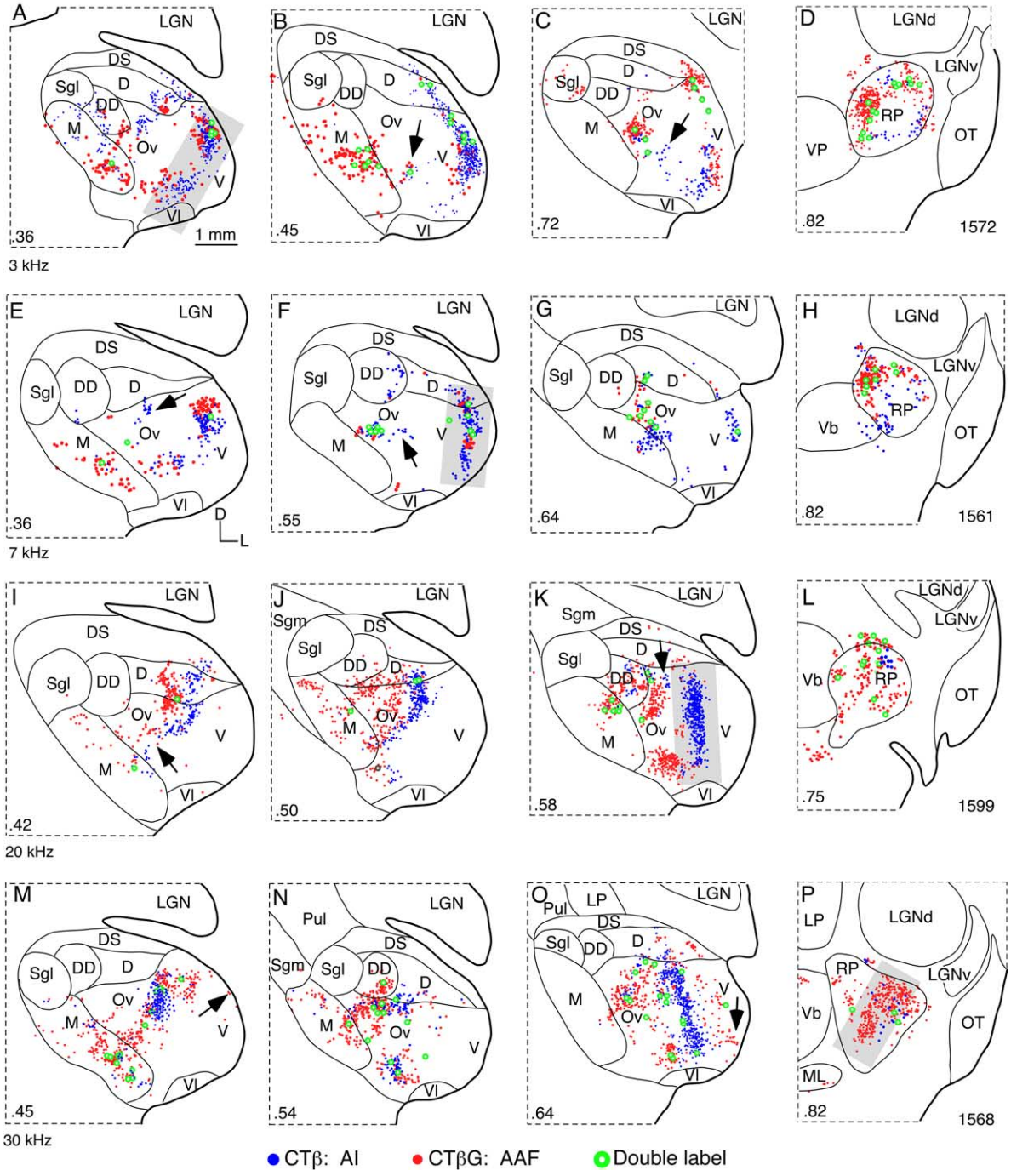

Fig. 2. Pattern of thalamic retrograde labeling in four cases: (A–D) 3 kHz, (E–H) 7 kHz, (I–L) 20 kHz, (M–P) 30 kHz. Neurons projecting to AI (blue dots) and AAF (red dots) are clustered and involve several nuclei. Neurons projecting to AI form dorsoventrally elongated strips in the ventral division that shift progressively lateromedially for higher frequency injections (A, F, K, O). AAF neurons are concentrated in the rostral pole and show a similar frequency shift dorsoventrally (D, H, L, P). Gray boxes in panels A, F, K, P illustrate examples of homotopic projections. Outside of the main groups of labeled cells, heterotopic projections arise from unexpected locations several millimeters away from the main clusters in the ventral and rostral pole divisions, and from the non-tonotopic nuclei of the dorsal and medial divisions (B, C, E, F, I, K, M, O: arrows). Few cells (green dots), approximately 1.6%, were double labeled. Decimals, percentage distance from caudal pole of the medial geniculate body; numbers on right refer to specific cases.

compared with the limits of the injected frequency regions in the Voronoi-Dirichlet tessellations; in every instance this territory fell within these boundaries, except for the 7 kHz experiment (Fig. 1B), where the physiological map was incomplete. In addition, the proportion of cells originating from non-tonotopic regions was also quantified as an additional source of heterotopic input (Reale and

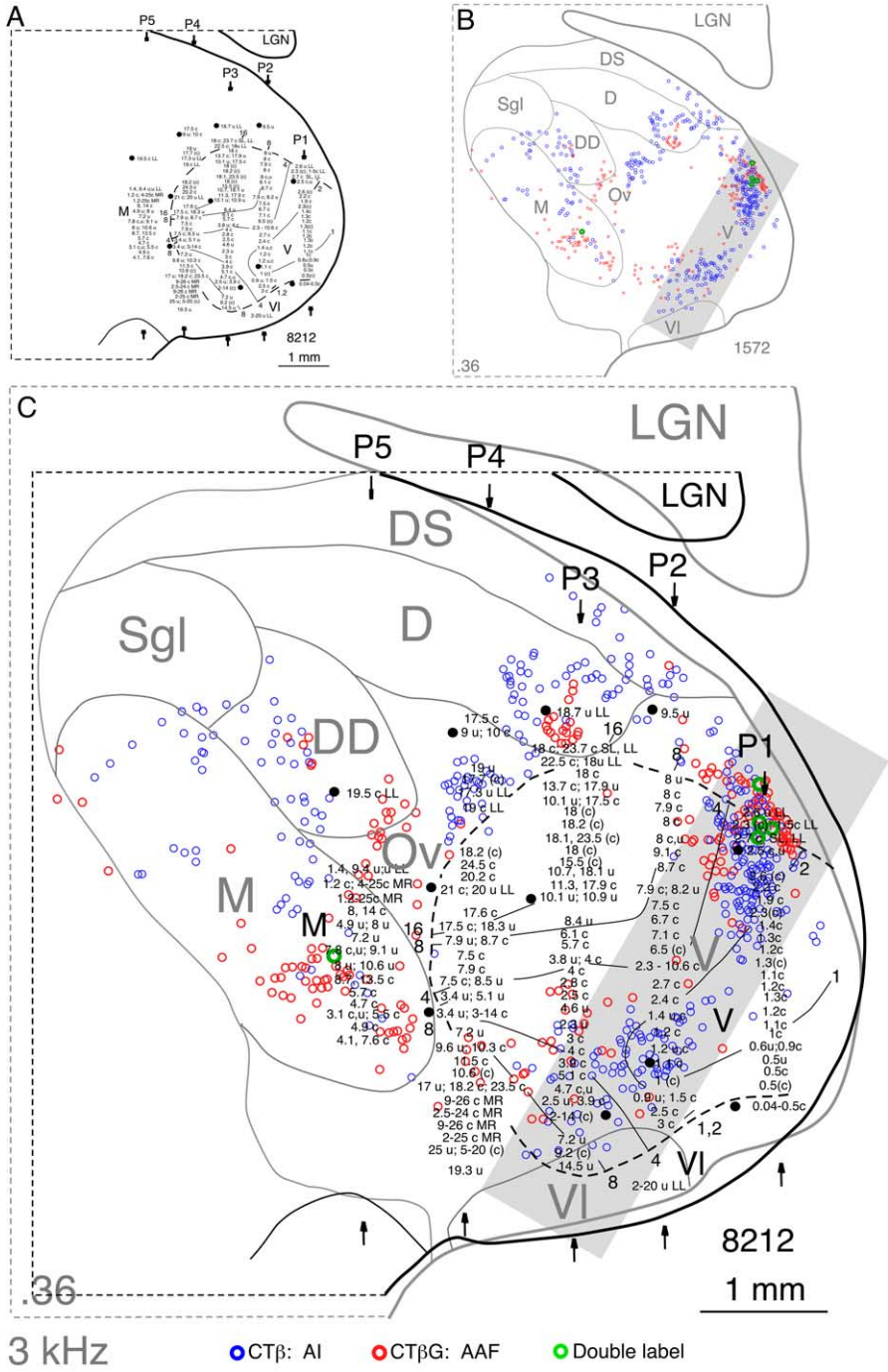

Fig. 3. Comparison of the distribution of thalamocortical retrograde labeling with medial geniculate body (MGB) tonotopic organization. (A) Physiological map of CF in the ventral division of the MGB redrawn from Imig and Morel, (1985), Fig. 6. (B) Thalamic labeling (colored dots in gray contour) from Fig. 2A from a closely corresponding section at a similar anteroposterior level from a cat medial geniculate body that had not been mapped physiologically. The limits of the homotopic region are indicated by the gray boxes in panels B, C. (C) Superimposition of panels A, B. The physiological map (black) includes five electrode tracts (P1–P5); filled black dots indicate marking lesions in the mapped thalamus, continuous internal lines correspond to putative isofrequency representations. Alignment of labeling was based on physical landmarks and the injection sites. Projections to the 3 kHz regions in AI (blue dots on the gray) and AAF (red dots on the gray) overlap with corresponding best-frequencies in the ventral division of the physiologically mapped thalamus. Heterotopic projections originated from sites up to three octaves away in the ventral division. Some neurons in medial and dorsal division structures also were misaligned with respect to frequency. Original figure modified and reproduced with permission.

Imig, 1980; Schreiner and Cynader, 1984; Clarey and Irvine, 1986; Rouiller et al., 1991; He et al., 1997).

We also compared these regions to contemporary physiological maps of the CF distribution in both the medial geniculate body (Imig and Morel, 1985) and the primary auditory cortex (Merzenich et al., 1975; Reale and Imig, 1980). In these instances the thalamic section or reconstructed cortex best matching the most complete map of medial geniculate body or auditory cortex was superimposed on the prior, physiological representation. For the auditory thalamus, the center of the labeling was aligned to the frequency distribution best matching the injected frequency in the cortical Voronoi-Dirichlet tessellation. For ipsilateral auditory cortex, the retrograde labeling was superimposed on the tessellation map based on the recorded location of injection sites and anatomical landmarks (Fig. 5). In the contralateral cortex, two methods were employed. Either the Voronoi-Dirichlet tessellation from the ipsilateral hemisphere or, alternatively, an analogous map from the literature (Merzenich et al., 1975; Reale and Imig, 1980) was superimposed such that the center of the deposit site and the CF representation were aligned with the center of the densest commissural labeling. Despite the interhemispheric and individual variability of maps, both approaches yielded similar results. The homo- and heterotopic labeling (Bianki et al., 1988) was identified by the same procedure as in the ipsilateral hemisphere.

RESULTS

Deposit sites

Physiological recordings in AI (Merzenich et al., 1975) and AAF (Knight, 1977) demonstrated the expected tonotopic arrangement of CF across the cortex. However, low to mid-frequencies (1–5 kHz) in AAF were underrepresented (Imaizumi et al., 2004). This difference supports the notion of parallel streams of CF processing in these areas (Lee et al., 2004). In AI and AAF, an octave was represented physically by a contour with a width of approximately 500–1000 μm, a value that in AAF was compressed to approximately 30% of the AI value. The physiological maps guided the focal injection of retrograde tracers, CTβ and CTβG, into matching low- (Fig. 1A), mid- (Fig. 1B, C), or high-frequency (Fig. 1D) subregions in both areas. Tracer spread was 250–1000 μm in diameter in all experiments and the ensuing deposit was confined entirely within an octave of the targeted frequency (Fig. 1A–D). The effective uptake of the deposit was approximately 500 μm or less (Fig. 1E: core). The resulting labeling included unexpected sources of convergent projections to these frequency-specific loci from anisotropic sources in the thalamus, ipsilateral cortex, and commissural cortex. This input originated well beyond the expected site of similar best-frequency within tonotopic thalamic nuclei and cortical areas, and from multiple non-tonotopic thalamic nuclei and cortical areas.

Thalamic projections

Thalamic projections to AI and AAF originated mainly from tonotopically appropriate parts of the ventral and rostral pole nuclei (Fig. 2). Thus, many ventral division neurons projecting to AI formed strips elongated dorsoventrally (Fig. 2: blue dots). These were centered caudolaterally in lower frequency cases (Fig. 2B, F; 3, 7 kHz) and rostromedially in higher frequency cases (Fig. 2K, O; 20, 30 kHz). Fewer neurons projected to AAF from the ventral division and they formed partially overlapping clusters at the dorsal and ventral extremes of these strips (Fig. 2: red dots), where a few double-labeled cells (<3%; Fig. 1G) projected to both areas (Fig. 2: green dots). In the rostral pole, overlapping clusters of cells projecting to both areas shifted from a dorsomedial position in the lower frequency cases (Fig. 2D, H) to a ventrolateral position in the higher frequency experiments (Fig. 2L, P).

Despite the global alignment of these projections with their expected locations, many of the thalamic neurons were in tonotopically inappropriate (heterotopic) locations,

Abbreviations used in the figures

AAF	anterior auditory field
AES	anterior ectosylvian sulcus
AI	primary auditory cortex
AII	secondary auditory cortical area
AS, c	cluster of units response
(c)	low-amplitude unit cluster response
CF	characteristic frequency
Cg	cingulate gyrus
CTβ	cholera toxin beta subunit
CTβG	cholera toxin beta subunit gold conjugate
D	dorsal nucleus of the medial geniculate body
DD	deep dorsal nucleus of the medial geniculate body
DS	dorsal superficial nucleus of the medial geniculate body
EPD	posterior ecosystem gyrus, dorsal part
EPI	posterior ecosystem gyrus, intermediate part
EPV	posterior ectosylvian gyrus, ventral part
Ins	insular cortex
LGN	lateral geniculate nucleus
LGNd	dorsal lateral geniculate nucleus
LGNv	ventral lateral geniculate nucleus
LL	long latency response
LP	lateral posterior nucleus
M	medial division of the medial geniculate body
MR	multiple frequency range
mss	middle suprasylvian sulcus
OT	optic tract
Ov	*pars ovoidea* of the medial geniculate body
P	posterior auditory cortex
pes	posterior ectosylvian sulcus
Pul	pulvinar
RP	rostral pole division of the medial geniculate body
SF	suprasylvian fringe auditory cortex (dorsal zone)
Sgl	suprageniculate nucleus, lateral part
Sgm	suprageniculate nucleus, medial part
SII	second somatic sensory area
SL	short-latency response
Te	temporal cortex
u	single unit response
V	ventral division of the medial geniculate body
Vb	ventrobasal complex
Ve	ventral auditory area
Vl	ventrolateral nucleus of the medial geniculate body
VP	ventral posterior auditory area
35/36	parahippocampal areas 35 and 36

Table 1. Heterotopic labeling in the ventral division of the medial geniculate body

Frequency	Experiment	AAF	AI
3 kHz	1572	11[1]	10
7 kHz	1561	28	28
20 kHz	1599	19	9
30 kHz	1568	23	4
Mean±S.E.		20±4	13±5

[1] Percentage.

up to 3 mm from the main cluster in the ventral division and up to 1 mm in the rostral pole. The proportion of heterotopic labeling in the ventral division represented 13±5% of the input to AI and 20±4% of the input to AAF (Table 1). In reconciling the thalamic labeling with contemporary physiological maps (Imig and Morel, 1985; see Discussion), the homotopic labeling clustered tightly with expected best frequency locations, while the heterotopic neurons (Fig. 3B) aligned with best frequencies as far as three octaves from the injected/predicted frequency (Fig. 3A, C). In addition to heterotopic projections within the tonotopic nuclei, 17–25% of the projections to AI and AAF originated from non-tonotopic medial geniculate body nuclei (Aitkin and Dunlop, 1968; Winer and Morest, 1983), mainly in the nuclei of the dorsal and medial division (Table 2). While these nuclei may have a coarse representation of the matching frequency (Rouiller et al., 1989), comparison with physiological maps suggested that, even in these nuclei, unmatched heterotopic frequency loci project to each area (Fig. 3). Double-labeled cells in all experiments were rare, approximately 1.6% of the total. These were scattered throughout the projection with no obvious segregation.

Corticocortical projections

The results were similar in the ipsilateral cortex (Fig. 4). Both AI and AAF receive the bulk of their projections from homotopic neurons within an area, whereas input from adjoining areas was nearly an order of magnitude weaker. Projections from the tonotopic areas (posterior auditory cortex, P, ventral posterior auditory area, VP, ventral auditory area, Ve) and other (secondary auditory cortical area, AII) regions predominated, with progressively weaker input from the posterior ectosylvian areas (posterior ectosylvian gyrus, dorsal part, EPD; posterior ectosylvian gyrus, intermediate part, EPI; posterior ectosylvian gyrus, ventral part, EPV), the suprasylvian fringe, SF, limbic and association areas (temporal cortex, Te, insular cortex, Ins, anterior ectosylvian sulcus, aes), and the cingulate, Cg and parahippocampal areas

Table 2. Origin of thalamic projections to AAF and AI

Area	Tonotopic nuclei	Non-tonotopic nuclei
AAF	74.7[1]	25.3
AI	82.6	17.4

[1] Percentage.

Table 3. Heterotopic ipsilateral projections

Frequency	Experiment	AAF	AI
3 kHz	1572	35[1]	33
7 kHz	1561	16	31
20 kHz	1599	17	32
30 kHz	1568	37	21
Mean±S.E.		26±6	29±3

[1] Percentage.

35, 36 (Lee et al., 2004); Fig. 4; vertical aliasing is an artifact of reconstruction). Again, projections from tonotopic areas originated largely from predicted homotopic locations in each area. Thus, as the injection sites shifted from low- to high-frequency in AI and AAF, partially overlapping clusters of labeling shift in another tonotopic region, e.g. from dorsal to ventral sectors in the posterior field (Fig. 4A, P). Again, double-labeled cells were rare (approximately 1.1%). Many labeled heterotopic neurons (>25%; Table 3) were well outside their predicted, frequency-matched locations in these areas, in some cases up to 6 mm away (Fig. 4A: arrow). Alignment of the intrinsic labeling with the experimentally determined physiological map confirmed that neurons up to three octaves away projected to a heterotopic locus (Fig. 5). Perhaps even more unexpected was the massive convergence of input from non-tonotopic areas, which composed 17–25% of the extrinsic ipsilateral projection to each area. Although the nature of the information contained in these non-tonotopic sources is largely unknown, their frequency tuning likely is broader than that in the primary areas (Reale and Imig, 1980; Schreiner and Cynader, 1984; Rouiller et al., 1991; He et al., 1997).

Commissural cells of origin

The commissural projection likewise obeyed many of the same projection principles as the thalamocortical and corticocortical systems (Fig. 6). Each area received its main input (approximately 85%) from the homotopic area and a weaker, asymmetric projection from other regions (approximately 15%). The homotopic neurons arose from the predicted, tonotopically appropriate locations in caudal AI and rostral AAF for lower frequency injections (Fig. 6A, B), and in rostral AI and caudal AAF for higher frequency injections (Fig. 6C, D). The commissural AI projection was more tightly clustered than the commissural AAF projection, which often spanned almost 75% of the length of AAF. This

Table 4. Heterotopic commissural projections

Frequency	Experiment	AAF	AI
3 kHz	1572	20[1]	14
7 kHz	1561	33	24
20 kHz	1599	27	11
30 kHz	1568	30	15
Mean±S.E.		28±3	16±3

[1] Percentage.

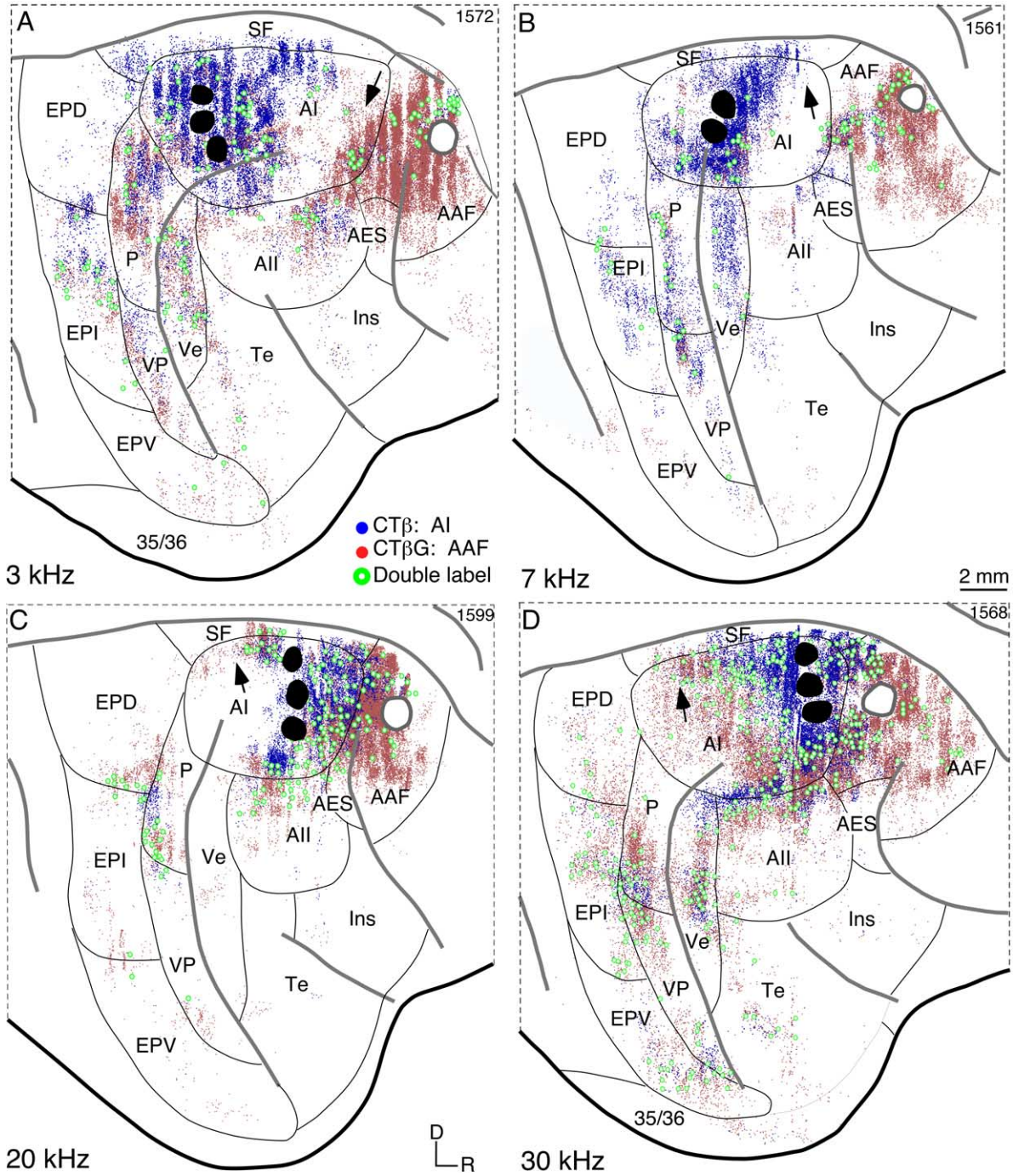

Fig. 4. Plots of the areal distribution of ipsilateral cortical projections to AI (blue dots) and AAF (red dots) after injecting retrograde tracers (black and white circles) at (A) 3 kHz, (B) 7 kHz, (C) 20 kHz, and (D) 30 kHz. Vertical banding of labeling is an artifact of the reconstruction from serial sections in the transverse plane projected onto a lateral view of the hemisphere. Tonotopically appropriate projections to AI and AAF originated from partially overlapping clusters in areas P, VP, and Ve. Significant heterotopic projections (arrows) arose in inappropriate locations in the tonotopic areas and from non-tonotopic fields, e.g. AII, EPI, SF, and they constitute approximately 30% of the extrinsic ipsilateral input. Neurons with branched projections (green dots) were sparse, approximately 1.1%.

was evident in an examination of the heterotopic labeling within each area, which was far larger in AAF (28±3%) than in AI (16±3%; Table 4). Alignment of the labeling with physiological maps from the ipsilateral hemisphere (Fig. 7A) or from prior work (Merzenich et al., 1975; Fig. 7B) similarly demonstrated that, while most of the labeling centered around the expected frequency location, heterotopic neurons in AI were labeled nearly three octaves away (Fig. 7: arrows). Once again, few double-labeled neurons were present (approximately 0.7%). Finally, sparse heter-

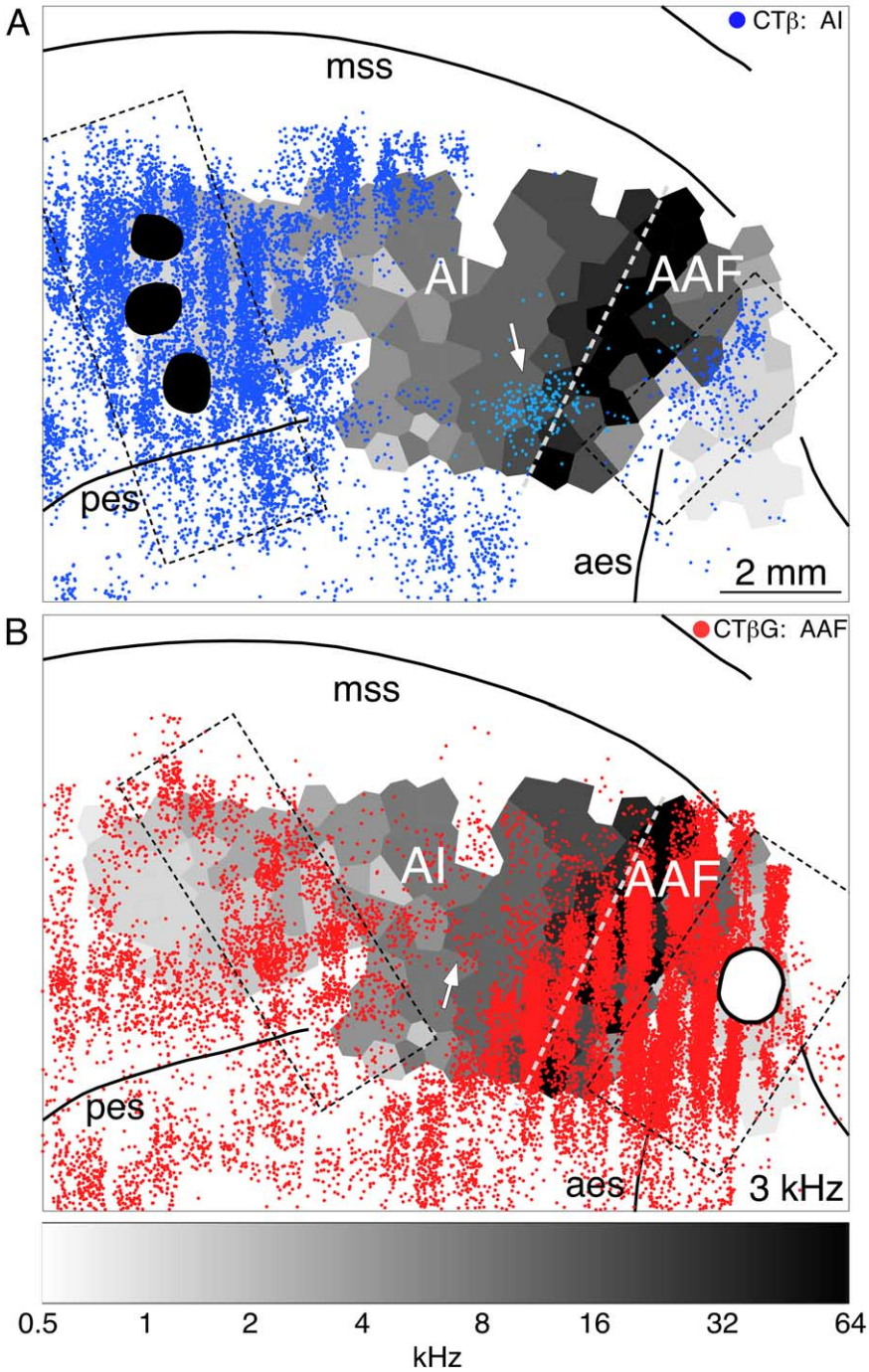

Fig. 5. Superimposition of the pattern of intrinsic retrograde labeling resulting from injections in AI (A, blue dots) and AAF (B, red dots) with the experimentally determined physiological map in the 3 kHz case (Fig. 1A). Vertical banding of labeling is an artifact of the reconstruction from serial sections. For clarity, the labeling from the AI (A) and AAF (B) injections are shown separately. Alignment was based on anatomical landmarks and injection sites. The labeling from the AI injections (A) clusters within 2 mm of the injection site and involves approximately 2.5 octaves. The limits of the homotopic regions are indicated by the dashed lines. Heterotopic labeling was found in AI and AAF from frequencies up to approximately 3 octaves away (arrows). The labeling from the AAF injection (B) spanned much of AAF, and heterotopic projections from subareas in AI and AAF were plentiful.

otopic projections also originated from non-tonotopic areas (AII, EPD, EPI). While these were slightly more prevalent in the low frequency cases (Fig. 6A, B), they comprised less than 5% of the commissural input.

Heterotopic projections thus are common in tonotopically inappropriate locations and non-tonotopic sources throughout the thalamus and the cortex. Their possible role is considered below.

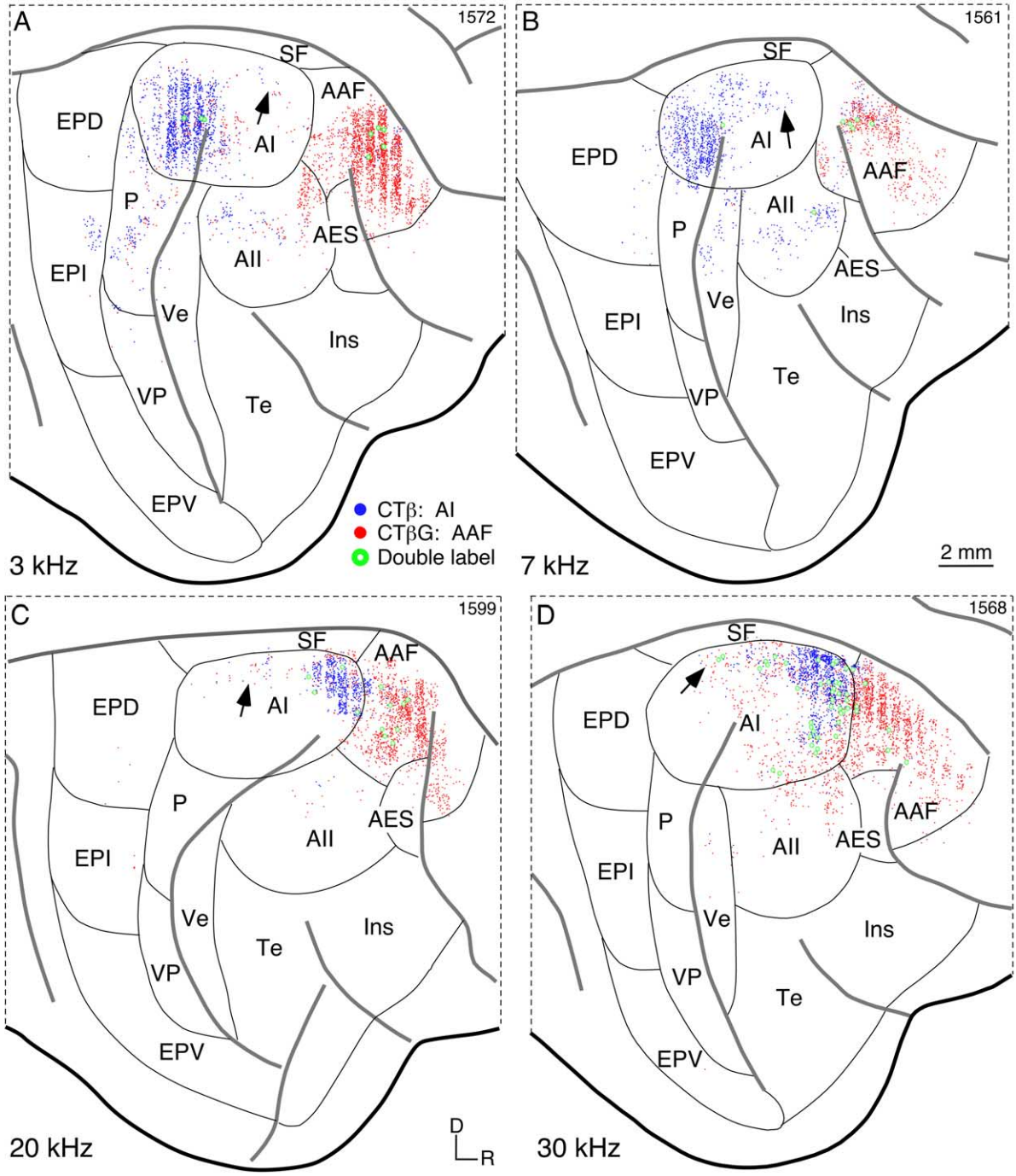

Fig. 6. Lateral view of plots of commissural projections to AI (blue dots) and AAF (red dots) in four experiments: (A) 3 kHz, (B) 7 kHz, (C) 20 kHz, (D) 30 kHz. Vertical banding of labeling is an artifact of the reconstruction from serial sections. To facilitate comparison, the orientation of the plots matches the ipsilateral orientation (cf. Fig. 4). In each experiment, the heaviest projection to AI and AAF originated from the homolateral area at tonotopically appropriate locations, while many heterotopic projections are found several millimeters away (arrows). The spread of labeling in AAF was larger and reflects an increase from heterotopic projections of approximately 175% relative to AI. Sparse projections from outside the homotopic areas originated mainly from other tonotopic areas, though there is significant AII labeling in almost all experiments. Double labeling (green dots) was approximately 0.7%.

DISCUSSION

We found significant projections to frequency-specific loci in AI and AAF from tonotopically inappropriate and non-tonotopic sources in the cortex and thalamus. These heterotopic projections might provide the essential input for the tonotopic loci to acquire new physiological properties and enable cortical map plasticity.

Methodological considerations

Perhaps the heterotopic labeling reflects inadvertent tracer diffusion outside of the target frequency or tracer uptake by

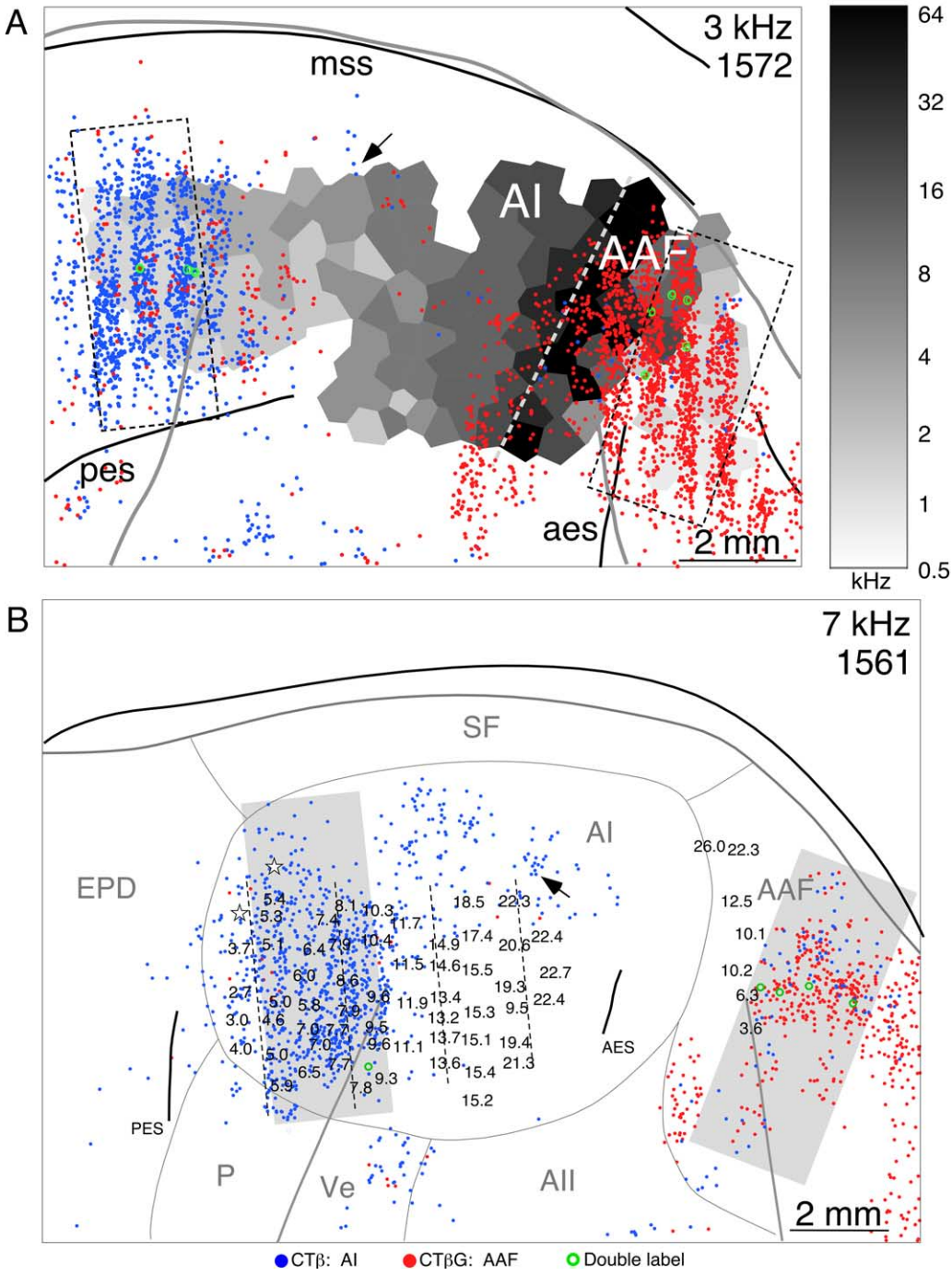

Fig. 7. Comparing retrograde commissural labeling and physiological maps in AI and AAF. Vertical banding of labeling is an artifact of the reconstruction from serial sections. (A) Superimposition and alignment of the commissural labeling from the 3 kHz case with the physiological map obtained from the ipsilateral hemisphere. (B) Alignments were also tested against maps from the contemporary literature, as shown in the best-fit of the 7 kHz case with the physiological map of CF in AI and in AAF by Merzenich et al. (1975) Fig. 1A, redrawn and reproduced with permission. Dashed lines in B indicate isofrequency contours in the original publication, and stars indicate lesion locations. Alignments were based on sulcal best-fits and the known injections sites. The center of the projections in AI (blue dots) and AAF (red dots) align closely with appropriate best frequencies (in black). The limits of the homotopic regions are indicated by the dashed lines (A) and gray boxes (B). The dispersion of labeling extends approximately 1.5 mm (less than two octaves). Heterotopic projections align with best frequencies up to three octaves away (arrows).

cut fibers. We believe that neither of these possibilities can account for our results. The tracers, CTβ and CTβG, were selected because they are highly sensitive (Llewellyn-Smith et al., 1990; Luppi et al., 1990; Ruigrok et al., 1995). Assessment of the injection sites demonstrates that the total tracer diffusion (deposit core plus all extracellular spread) is 500–1000 μm (Fig. 1A–F), which is within an octave of the targeted frequency (Merzenich et al., 1975;

Reale and Imig, 1981; Imig et al., 1982). It is unlikely that the size of the injections is underestimated systematically due to shrinkage from an extended survival or rapid transport or tracer clearance at the periphery, since the survivals were certainly too brief to permit disappearance of the deposit sites, and because much of the thalamic and cortical labeling is confined to tight clusters at their tonotopically appropriate locations. If tracer diffusion or incorporation by transected fibers were significant, one would expect a continuous distribution of retrogradely labeled cells to extend from the tonotopically appropriate clusters across multiple isofrequency contours in the thalamus and cortex. This is not the case. Instead, the heterotopic labeling is invariably focal, clustered, and separated from the main mass of labeling, sometimes by as much as 3 mm in the thalamus and 8 mm in the cortex, thus indicating that these projections are specific. In addition, our quantification of the heterotopic labeling considers only those projections originating outside a core area of 1 or 2 mm in width, spanning between one and two octaves in the thalamus (Imig and Morel, 1985) and cortex (Merzenich et al., 1975; Reale and Imig, 1980), respectively. This provides a generous margin for any extraneous labeling due to limitations of the tracers.

Comparison with prior studies

The present investigation is certainly not the first to have described heterotopic corticocortical (Matsubara and Phillips, 1988) or thalamocortical (Morel and Imig, 1987) connectivity among tonotopic representations in the auditory forebrain. Indeed, analysis of the 'complete' representation of a 10 kHz cortical isofrequency contour in the medial geniculate body using horseradish peroxidase suggests an even more substantial heterotopic projection (Morel and Imig, 1987, their Fig. 7, p. 129) than that shown here for 7 and 20 kHz deposits, respectively. At the other extreme minute microdeposits confined to a subregion of an isofrequency laminae produce little if any medial geniculate labeling that would seem to be a candidate for heterotopic status (Brandner and Redies, 1990). This suggests that one structural basis for heterotopic projections is the intraareal dispersion of single thalamocortical fibers (Huang and Winer, 2000), though this remains to be demonstrated in auditory cortex as it has been in the visual (Ferster and LeVay, 1978) and somatic sensory (Landry and Deschênes, 1981) cortices. Moreover, there may be a scale for heterotopic connectivity that does not extend to the finest subdivisions of cortical representation. It seems probable that there is analogous divergence of corticocortical and commissural axons that could underlie their heterotopic contributions.

It is somewhat more problematic to compare the present results to prior tract tracing studies of auditory cortex since they used either less sensitive tracers (Winer et al., 1977), or tracers such as tritiated bovine serum albumin whose efficacy is not widely validated relative to CTβ fragment (Imig and Morel, 1984). Another investigation did not map auditory cortex at sufficiently high resolution to establish the origin of extrinsic projections (Andersen et al., 1980). Each of these factors makes the definitive determination of heterotopic labeling less secure and tempers any direct comparison between the various approaches. In the present study, high-resolution mapping coupled with the focal deposit of highly sensitive tracers reveals the extent of homotopic and heterotopic sources with the fidelity necessary for the quantitative assessment of their number. The new findings in the present study include common metrics for heterotopic origins in the thalamus and cerebral cortex, and the demonstration of heterotopic connectivity in two primary fields that suggests it is a global principle of auditory forebrain organization.

Parallel pathways

An important principle in the contemporary neuroscience of vision, somatic sensation, and audition is that peripheral sensory receptor subtypes are represented by parallel processing streams in the brain. Thus, retinal X, Y, and W ganglion cells segregate the input from rods and cones, respectively, before propagating it to the lateral geniculate nucleus (Sur et al., 1987) and the superior colliculus (Berson et al., 1990), respectively. Even within the cerebral cortex, the distinction between form/color and motion/scotopic streams is preserved at sites remote from the retina (DeYoe et al., 1994). The somatic sensory system follows a similar principle, segregating the output of different classes of peripheral receptors both within the spinal cord and far higher in the neuraxis (Jones and Porter, 1980; Dykes, 1983). It is unknown how many functional streams exist in the auditory system (Romanski et al., 1999; Read et al., 2002). The paucity of subtypes of auditory receptors represents something of a departure from the several types of peripheral receptors in vision and somatic sensation. Thus, type I ganglion cells innervating inner hair cells represent more than 95% of the fibers in the auditory nerve (Kiang et al., 1965), reducing the parallel input from outer hair cells and their type II ganglion cells to a mere fraction of the total and whose central representation is uncertain (Morest and Bohne, 1983). However, recent studies suggest that distinct functional processing streams may be already constituted at the level of the brainstem and remain segregated at the midbrain and, potentially, beyond (Ramachandran et al., 1999; Davis and Young, 2000).

The tonotopic organization of the primary auditory cortical areas appears to be a reflection of this segregation of frequencies in the cochlea that is propagated across multiple stations in the midbrain and thalamus (Winer, 1992). The representation of other functional streams within the tonotopic network has been shown for binaural properties (Middlebrooks and Zook, 1983; Velenovsky et al., 2003). In current models, this segregation is effected by strict point-to-point connections (Brandner and Redies, 1990) arranged in a hierarchical series (Rouiller et al., 1991). A strict model of parallel processing cannot readily account for the emergence of novel frequency representations during plastic rearrangements (Calford et al., 1993; Irvine and Rajan, 1997), since such information is clearly restricted to specific channels. Interactions between such parallel

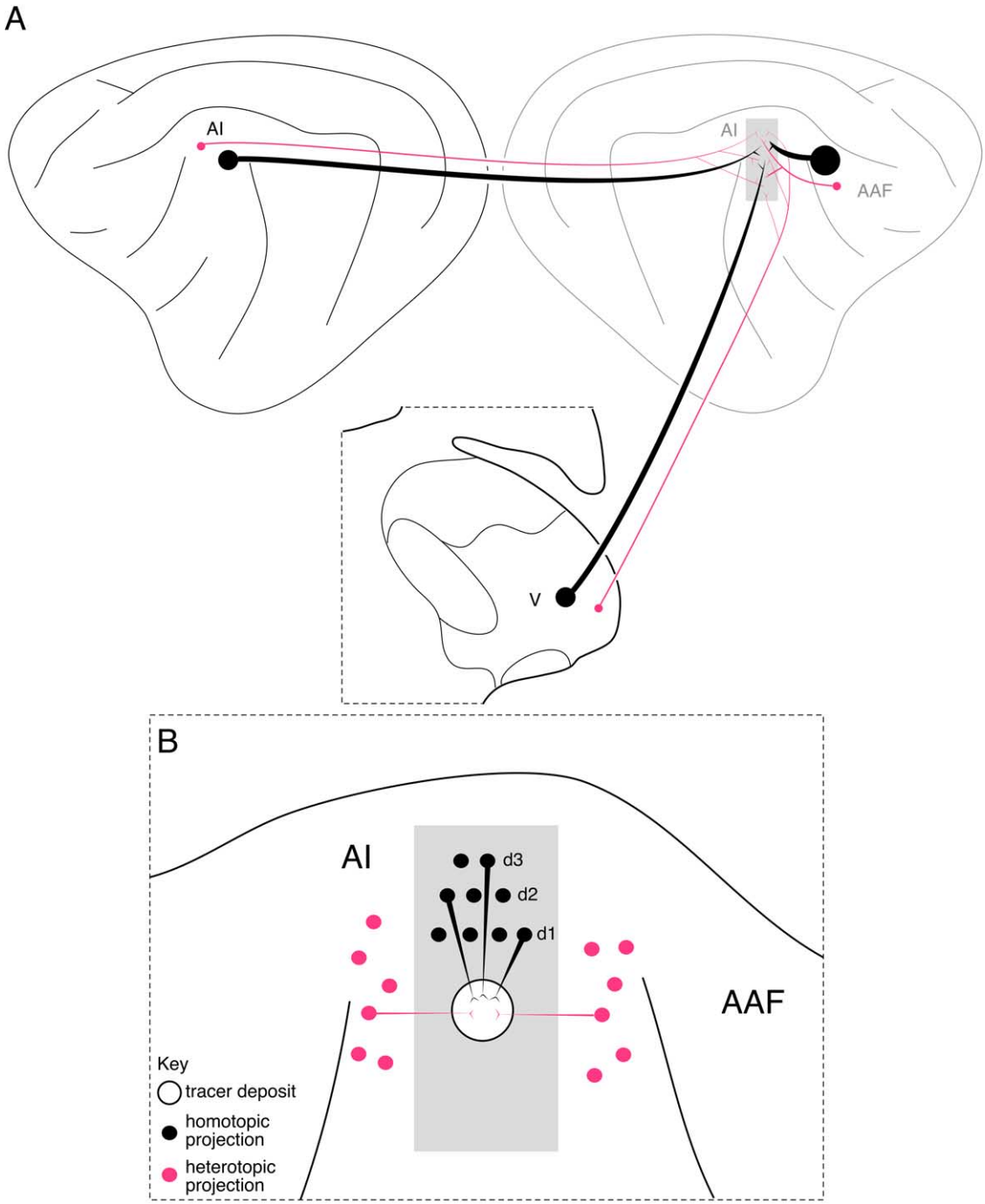

Fig. 8. Summary of a model of homotopic and heterotopic convergence onto an isofrequency contour (gray box) from (A) extrinsic sources in the thalamus, ipsilateral cortex, and the contralateral cortex and (B) intrinsic projections within an area. Size of circles is proportional to the numerical strength of connections; d1–d3 indicate modular homotopic connections among narrowband regions along an isofrequency contour (Read et al., 2001). The heterotopic projections permit CF representation beyond the classic frequency domain and could enable cortical map expansion during plasticity (see Discussion).

channels must occur for neurons to expand their signaling repertoire.

It is pertinent to point out that the role of the heterotopic system may not be limited to frequency-specific plasticity. Indeed, there is no a priori reason to expect it to be so restricted, and we offer the idea that it serves frequency-specific reorganization as only one of many possibilities. It is equally likely that such projections could contribute to or enhance receptive field properties outside the classic domain (Allman et al., 1985a,b) or play a role in global processes extending far from the CF or receptive field center (Angelucci et al., 2002). Still other alternatives in-

clude a contribution to binding (Treisman, 1999) or to cortical processes that require concerted horizontal intracortical connectivity (Gilbert, 1985; Das and Gilbert, 1995; Kisvárday et al., 1996; Kubota et al., 1997; Sutter et al., 1999; Read et al., 2001). One rationale for proposing a role in the frequency domain was that such reorganizations might be elicited from processes in the thalamus, ipsilateral cortex, or contralateral hemisphere. Irrespective of what roles heterotopic projections ultimately have, they are certainly appropriate candidates for providing essential input for rapid frequency-specific reorganization.

Role of branched projections

A correlate of the variety of peripheral receptors is that multiple sensory maps are the rule in many modalities. In the visual (Ferster and LeVay, 1978) and somatic sensory (Landry and Deschênes, 1981) systems, thalamic neurons with branched axons could contribute to the emergence of new maps or the elaboration of the single receptor epithelium in the cortex. In the auditory system, axonal branching is the rule in the cochlear nucleus via the division of auditory nerve fibers (Lorente de Nó, 1933), and in the divergent distribution of its output axons to the superior olivary complex (Schofield, 1995), trapezoid body (Friauf and Ostwald, 1988), lateral lemniscal nuclei (Schofield and Cant, 1997), and inferior colliculus (Oliver, 1984). Single thalamocortical arbors appear limited to zones of approximately 500–1000 μm, predominantly elongated along the isofrequency contour (Huang and Winer, 2000; Velenovsky et al., 2003). Retrograde tracer injections in different frequency regions separated by up to 3 mm within AI have shown a sparse (approximately 0.5%) population of neurons projecting to both loci (Lee and Winer, 2001). This apparent paucity of branching across frequencies suggests a limited role for these projections as substrates for reorganization, in comparison with the relatively robust heterotopic projections. However, the possibility remains that the few such divergent cells present might contribute to an intercortical process requiring temporally coordinated input, such as combination sensitivity, which may occur in some form in felines (Gehr et al., 2000) but whose neural basis is unknown. In any case, the paucity of such cells is enigmatic and suggests fundamental differences in input segregation relative to the brainstem. This is in contrast to the many thalamic neurons that project to cortex as well as to the thalamic reticular nucleus (Pinault and Deschênes, 1998) and it supports the idea that thalamic projections to different sensory neocortical areas maybe far more common in the feline visual system (Humphrey et al., 1985b) than in auditory forebrain.

Other possible sources for global reorganization

This model suggests that a substantial portion of the information required for establishing remapped parameters during plastic rearrangements could arise from the heterotopic projections in the thalamus and cortex. However, multiple projection systems outside of those ascending through the thalamus are capable of influencing the activity of the cortex and thus could provide potential substrates for reorganization. These include diffuse projections from nuclei in the brainstem reticular formation which supply cholinergic (Mesulam et al., 1983), serotonergic (Wilson and Molliver, 1991), histaminergic (Saper, 1985), and noradrenergic (Levitt and Moore, 1979) innervation, as well as direct projections to the auditory thalamus from the cochlear nucleus (Malmierca et al., 2002). While each of the chemically specific systems can influence broad cortical territories (Descarries et al., 1975, 1977), their effects are largely modulatory (Cooper et al., 1991) and thus, we propose, inherently unsuitable for eliciting rapid, global and precise reorganization in the frequency domain. As in the case of nucleus basalis stimulation (Kilgard and Merzenich, 1998), activating these systems might trigger the shift between cortical states, and could thus enable the expression of the information contained within the heterotopic projections (Steriade and Llinás, 1988; McCormick et al., 1993).

Projections from the cortex to the thalamic reticular nucleus may also play a role in reorganizing cortical parameters via cortico-thalamo-cortical interactions (Conley et al., 1991; Crabtree, 1998). The thalamic reticular nucleus is the source of potent GABAergic input to the thalamus (Bickford et al., 2000), and it has been proposed to modulate state dependent switching between tonic and burst modes of firing in thalamic neurons (Sherman and Guillery, 1998). Such state-dependent switches during plastic processes may induce heterotopic thalamic neurons to express functional connectivity in remapping the cortex.

Interneuronal connections within the auditory cortex (Prieto et al., 1994) could provide another necessary element in this process. The information from the heterotopic projections may normally be suppressed or masked via these inhibitory connections (Abeles and Goldstein, 1972) and, thus, invisible during physiological recording (Schreiner and Sutter, 1992; Gaese and Ostwald, 2001). During the activation of plastic rearrangements, the tonic inhibition of such heterotopic subsystems could be released.

The interaction of several neuronal systems may contribute to the expression of the information contained in the heterotopic projections during plastic rearrangements. Whether these heterotopic projections are involved in this process remains a question for further study.

Possible role of heterotopic projections

The heterotopic projection system in the thalamus and cortex satisfies several criteria that may be necessary for the plastic rearrangement of cortex (Winer et al., 2004). First, these heterotopic projections are present in the thalamic, corticocortical, and commissural connections. It seems unlikely that such a system of projections could exist in one but not all systems, since the remapped parameters must embody the convergent input from all of these systems (Fig. 8), and should also be propagated, supported, and coordinated throughout the entire network. Thus, similar and related heterotopic projections in each system (Lee et al., 2004) may be required to maintain

coherence and to synchronize remapped information across the network.

Second, heterotopic projections occur in thalamic nuclei and cortical areas with or without tonotopy. In the tonotopic nuclei and areas, these projections originate from tonotopically inappropriate locations. In the non-tonotopic loci, these projections may provide coarse intrinsic representations of frequencies that might subserve remapping. If one set of connections were excluded, perhaps the dynamic range of remapped properties that are achievable would be reduced concomitantly, and perhaps the totality of extrinsic heterotopic connections is a metric of the total cortical capacity for reorganization.

Finally, these heterotopic projections are sufficiently large and ubiquitous to plausibly support such rearrangements. They comprise >10% of the projections in each system, and may be as large as 29%. Indeed, given our conservative criterion for assessing their number, they might well be substantially larger than we estimate. If such projections were too sparse, their ability to influence cortical parameters would likely be weak or attenuated. If the projections were larger, one would expect to see a constitutive expression of their information and a remapping that is elicited even more readily than that presumably driven by nucleus basalis-induced plasticity. The magnitude of these projections is reasonable for providing the necessary input observed in the remapping experiments. It remains for future work to specify the role that these projections play in cortical plasticity and physiology.

Acknowledgments—Thanks to Ms Poppy Crum, Mr. Andrew Tan, and Dr. Bénédicte Philibert for assistance in the physiological recordings. Mr. David T. Larue and Ms Tania J. Bettis provided histological expertise. These studies were supported by National Institutes of Health grants R01 DC2260-04 and P01 NS3485 (C.E.S.) and R01 DC2319-24 (J.A.W.).

REFERENCES

Abeles M, Goldstein MH Jr (1972) Responses of single units in the primary auditory cortex of the cat to tones and to tone pairs. Brain Res 42:337–352.

Adams JC (1981) Heavy metal intensification of DAB-based HRP reaction product. J Histochem Cytochem 29:775.

Aitkin LM, Dunlop CW (1968) Interplay of excitation and inhibition in the cat medial geniculate body. J Neurophysiol 31:44–61.

Allman J, Miezin F, McGuinness E (1985a) Direction- and velocity-specific responses from beyond the classical receptive field in the middle temporal visual area (MT). Perception 14:105–126.

Allman J, Miezin F, McGuinness E (1985b) Stimulus specific responses from beyond the classical receptive field: neurophysiological mechanisms for local-global comparisons in visual neurons. Annu Rev Neurosci 8:407–430.

Andersen RA, Knight PL, Merzenich MM (1980) The thalamocortical and corticothalamic connections of AI, AII, and the anterior auditory field (AAF) in the cat: evidence for two largely segregated systems of connections. J Comp Neurol 194:663–701.

Angelucci A, Levitt JB, Walton EJS, Hupé J-M, Bullier J, Lund JS (2002) Circuits for local and global signal integration in primary visual cortex. J Neurosci 22:8633–8646.

Berson DM, Lu J, Stein JJ (1990) Topographic variations in W-cell input to cat superior colliculus. Exp Brain Res 79:459–466.

Bianki VL, Bozhko GT, Slepchenko AF (1988) Interhemispheric asymmetry of homotopic transcallosal responses of the auditory cortex in the cat. Neurosci Behav Physiol 18:315–323.

Bickford ME, Ramcharan E, Godwin DW, Erişir A, Gnadt J, Sherman SM (2000) Neurotransmitters contained in the subcortical extraretinal inputs to the monkey lateral geniculate nucleus. J Comp Neurol 424:701–717.

Brandner S, Redies H (1990) The projection of the medial geniculate body to field AI: organization in the isofrequency dimension. J Neurosci 10:50–61.

Bullier J, Kennedy H, Salinger W (1984) Bifurcation of subcortical afferents to visual areas 17, 18, and 19 in the cat cortex. J Comp Neurol 228:308–328.

Calford MB (2002) Dynamic representational plasticity in sensory cortex. Neuroscience 111:709–738.

Calford MB, Rajan R, Irvine DRF (1993) Rapid changes in the frequency tuning of neurons in cat auditory cortex resulting from pure-tone-induced temporary threshold shift. Neuroscience 55:953–964.

Campbell MJ, Morrison JH (1989) Monoclonal antibody to neurofilament protein (SMI-32) labels a subpopulation of pyramidal neurons in the human and monkey neocortex. J Comp Neurol 282:191–205.

Clarey JC, Irvine DRF (1986) Auditory response properties of neurons in the anterior ectosylvian sulcus of the cat. Brain Res 386:12–19.

Conley M, Kupersmith AC, Diamond IT (1991) The organization of projections from subdivisions of the auditory cortex and thalamus to the auditory sector of the thalamic reticular nucleus in *Galago*. Eur J Neurosci 3:1089–1103.

Cooper JR, Bloom FE, Roth RH (1991) The biochemical basis of neuropharmacology. New York: Oxford University Press.

Crabtree JW (1998) Organization in the auditory sector of the cat's thalamic reticular nucleus. J Comp Neurol 390:167–182.

Das A, Gilbert CD (1995) Long-range horizontal connections and their role in cortical reorganization revealed by optical recording of cat primary visual cortex. Nature 375:780–784.

Davis KA, Young ED (2000) Pharmacological evidence of inhibitory and disinhibitory neuronal circuits in dorsal cochlear nucleus. J Neurophysiol 83:926–940.

Descarries L, Beaudet A, Watkins KC (1975) Serotonin nerve terminals in adult rat neocortex. Brain Res 100:563–588.

Descarries L, Watkins KC, Lapierre Y (1977) Noradrenergic axon terminals in the cerebral cortex of rat: topometric ultrastructural analysis. Brain Res 133:197–222.

DeYoe EA, Felleman DJ, Van Essen DC, McClendon E (1994) Multiple processing streams in occipitotemporal visual cortex. Nature 371:151–154.

Dykes RW (1983) Parallel processing of somatosensory information: a theory. Brain Res Brain Res Rev 6:47–115.

Ferster D, LeVay S (1978) The axonal arborizations of lateral geniculate neurons in the striate cortex of the cat. J Comp Neurol 182:923–944.

Friauf E, Ostwald J (1988) Divergent projections of physiologically characterized rat ventral cochlear nucleus neurons as shown by intra-axonal injection of horseradish peroxidase. Exp Brain Res 73:263–284.

Gaese BH, Ostwald J (2001) Anesthesia changes frequency tuning of neurons in the rat primary auditory cortex. J Neurophysiol 86:1062–1066.

Galvan VV, Weinberger NM (2002) Long-term consolidation and retention of learning-induced plasticity in the auditory cortex of the guinea pig. Neurobiol Learn Mem 77:78–108.

Gehr DD, Komiya H, Eggermont JJ (2000) Neuronal responses in cat primary auditory cortex to natural and altered species-specific calls. Hearing Res 150:27–42.

Gilbert CD (1985) Horizontal integration in the neocortex. Trends Neurosci 8:160–165.

He J, Hashikawa T, Ojima H, Kinouchi Y (1997) Temporal integration and duration tuning in the dorsal zone of cat auditory cortex. J Neurosci 17:2615–2625.

Huang CL, Larue DT, Winer JA (1999) GABAergic organization of the cat medial geniculate body. J Comp Neurol 415:368–392.

Huang CL, Winer JA (2000) Auditory thalamocortical projections in the cat: laminar and areal patterns of input. J Comp Neurol 427:302–331.

Humphrey AL, Sur M, Uhlrich DJ, Sherman SM (1985a) Projection patterns of individual X- and Y-cell axons from the lateral geniculate nucleus to cortical area 17 in the cat. J Comp Neurol 233:159–189.

Humphrey AL, Sur M, Uhlrich DJ, Sherman SM (1985b) Termination patterns of individual X- and Y-cell axons in the visual cortex of the cat: projections to area 18, to the 17/18 border region, and to both areas 17 and 18. J Comp Neurol 233:190–212.

Imaizumi K, Priebe NJ, Crum PAC, Bedenbaugh PH, Cheung SW, Schreiner CE (2004) Modular functional organization of cat anterior auditory field. J Neurophysiol 92:444–457.

Imig TJ, Morel A (1984) Topographic and cytoarchitectonic organization of thalamic neurons related to their targets in low-, middle-, and high-frequency representations in cat auditory cortex. J Comp Neurol 227:511–539.

Imig TJ, Morel A (1985) Tonotopic organization in ventral nucleus of medial geniculate body in the cat. J Neurophysiol 53:309–340.

Imig TJ, Reale RA (1981) Ipsilateral corticocortical projections related to binaural columns in cat primary auditory cortex. J Comp Neurol 203:1–14.

Imig TJ, Reale RA, Brugge JF (1982) The auditory cortex: patterns of corticocortical projections related to physiological maps in the cat. In: Cortical sensory organization, Vol. 3: multiple auditory areas (Woolsey CN, eds), pp 1–41. Clifton, NJ: Humana Press.

Irvine DRF, Rajan R (1997) Injury-induced reorganization of frequency maps in adult auditory cortex: the role of unmasking of normally-inhibited inputs. Acta Otolaryngol (Stockholm) Supplement 532:39–45.

Jacobs KM, Donoghue JP (1991) Reshaping the cortical motor map by unmasking latent intracortical connections. Science 251:944–947.

Jones EG, Porter R (1980) What is area 3a? Brain Res Brain Res Rev 2:1–43.

Kaas JH (1997) Topographic maps are fundamental to sensory processing. Brain Res Bull 44:107–112.

Kennedy H, Bullier J (1985) A double-labelling investigation of the afferent connectivity to cortical areas VI and V2 of the macaque monkey. J Neurosci 5:2815–2830.

Kiang NY-S, Watanabe T, Thomas EC, Clark LF (1965) Discharge patterns of single fibers in the cat's auditory nerve. Cambridge, MA: MIT Press.

Kilgard MP, Merzenich MM (1998) Cortical map reorganization enabled by nucleus basalis activity. Science 279:1714–1718.

Kisvárday ZF, Bonhoeffer T, Kim D-S, Eysel UT (1996) Functional topography of horizontal neuronal networks in cat visual cortex (area 18). In: Brain theory: biological basis and computational principles (Aertsen A, Braitenberg V, eds), pp 97–122. Amsterdam: Elsevier.

Knight PL (1977) Representation of the cochlea within the anterior auditory field (AAF) of the cat. Brain Res 130:447–467.

Kubota M, Sugimoto S, Horikawa J, Nasu M, Taniguchi I (1997) Optical imaging of dynamic horizontal spread of excitation in rat auditory cortex slices. Neurosci Lett 237:77–80.

Landry P, Deschênes M (1981) Intracortical arborizations and receptive fields of identified ventrobasal thalamocortical afferents to the primary somatic sensory cortex in the cat. J Comp Neurol 199:345–372.

Lee CC, Imaizumi K, Schreiner CE, Winer JA (2004) Concurrent tonotopic processing streams in auditory cortex. Cereb Cortex 14:441–451.

Lee CC, Winer JA (2001) The auditory thalamus: anatomical constraints governing cortical projections. Soc Neurosci Abstr 27:930

Levitt P, Moore RY (1979) Development of the noradrenergic innervention of neocortex. Brain Res 162:243–259.

Llewellyn-Smith IJ, Minson JB, Wright AP, Hodgson AJ (1990) Cholera toxin B-gold, a retrograde tracer that can be used in light and electron microscopic immunocytochemical studies. J Comp Neurol 294:179–191.

Lorente de Nó R (1933) Anatomy of the eighth nerve: the central projection of the nerve endings of the inner ear. Laryngoscope 43:1–38.

Luppi P-H, Fort P, Jouvet M (1990) Iontophoretic application of unconjugated cholera toxin B subunit (CTb) combined with immunohistochemistry of neurochemical substances: a method for transmitter identification of retrogradely labeled neurons. Brain Res 534:209–224.

Malmierca MS, Merchán MA, Henkel CK, Oliver DL (2002) Direct projections from cochlear nuclear complex to auditory thalamus in the rat. J Neurosci 22:10891–10897.

Matsubara JA, Phillips DP (1988) Intracortical connections and their physiological correlates in the primary auditory cortex (AI) of the cat. J Comp Neurol 268:38–48.

McCormick DA, Wang Z, Huguenard J (1993) Neurotransmitter control of neocortical neuronal activity and excitability. Cereb Cortex 3:387–398.

Merzenich MM, Knight PL, Roth GL (1975) Representation of cochlea within primary auditory cortex in the cat. J Neurophysiol 38:231–249.

Mesulam M-M, Mufson EJ, Wainer BH, Levey AI (1983) Central cholinergic pathways in the rat: an overview based on an alternative nomenclature (Ch1-Ch6). Neuroscience 10:1185–1201.

Middlebrooks JC, Zook JM (1983) Intrinsic organization of the cat's medial geniculate body identified by projections to binaural response-specific bands in the primary auditory cortex. J Neurosci 3:203–225.

Morel A, Imig TJ (1987) Thalamic projections to fields A, AI, P, and VP in the cat auditory cortex. J Comp Neurol 265:119–144.

Morest DK, Bohne BA (1983) Noise-induced degeneration in the brain and representation of inner and outer hair cells. Hearing Res 9:145–151.

Oliver DL (1984) Dorsal cochlear nucleus projections to the inferior colliculus in the cat: a light and electron microscopic study. J Comp Neurol 224:155–172.

Pinault D, Deschênes M (1998) Projections and innervation patterns of individual thalamic reticular axons in the thalamus of the adult rat: a three-dimensional, graphic, and morphometric analysis. J Comp Neurol 391:180–203.

Prieto JJ, Peterson BA, Winer JA (1994) Morphology and spatial distribution of GABAergic neurons in cat primary auditory cortex (AI). J Comp Neurol 344:349–382.

Rajan R, Irvine DRF, Wise LZ, Heil P (1993) Effect of unilateral partial cochlear lesions in adult cats on the representation of lesioned and unlesioned cochleas in primary auditory cortex. J Comp Neurol 338:17–49.

Ramachandran R, Davis KA, May BJ (1999) Single-unit responses in the inferior colliculus of decerebrate cats I. Classification based on frequency response maps. J Neurophysiol 82:152–163.

Read HL, Winer JA, Schreiner CE (2001) Modular organization of intrinsic connections associated with spectral tuning in cat auditory cortex. Proc Natl Acad Sci USA 98:8042–8047.

Read HL, Winer JA, Schreiner CE (2002) Functional architecture of primary auditory cortex. Curr Opin Neurobiol 12:433–440.

Reale RA, Imig TJ (1980) Tonotopic organization in auditory cortex of the cat. J Comp Neurol 182:265–291.

Recanzone GH, Schreiner CE, Merzenich MM (1993) Plasticity in the frequency representation of primary auditory cortex following discrimination training in adult owl monkeys. J Neurosci 13:87–103.

Romanski LM, Tian B, Fritz J, Mishkin M, Goldman-Rakic PS, Rauschecker JP (1999) Dual streams of auditory afferents target multiple domains in the primate prefrontal cortex. Nat Neurosci 2:1131–1136.

Rouiller EM, Rodrigues-Dagaeff C, Simm G, de Ribaupierre Y, Villa AEP, de Ribaupierre F (1989) Functional organization of the medial division of the medial geniculate body of the cat: tonotopic organization, spatial distribution of response properties and cortical connections. Hearing Res 39:127–146.

Rouiller EM, Simm GM, Villa AEP, de Ribaupierre Y, de Ribaupierre F (1991) Auditory corticocortical interconnections in the cat: evidence for parallel and hierarchical arrangement of the auditory cortical areas. Exp Brain Res 86:483–505.

Ruigrok TJH, Teune TM, van der Burg J, Sabel-Goedknegt H (1995) A retrograde double-labeling technique for light microscopy: a combination of axonal transport of cholera toxin B-unit and a gold-lectin conjugate. J Neurosci Methods 61:127–138.

Saper CB (1985) Organization of cerebral cortical afferent systems in the rat. II. Hypothalamocortical projections. J Comp Neurol 237:21–46.

Schieber MH (2001) Constraints on somatotopic organization in the primary motor cortex. J Neurophysiol 86:2125–2143.

Schofield BR (1995) Projections from the cochlear nucleus to the superior paraolivary nucleus in guinea pigs. J Comp Neurol 360:135–149.

Schofield BR, Cant NB (1997) Ventral nucleus of the lateral lemniscus in guinea pigs: cytoarchitecture and inputs from the cochlear nucleus. J Comp Neurol 379:363–385.

Schreiner CE, Cynader MS (1984) Basic functional organization of second auditory cortical field (AII) of the cat. J Neurophysiol 51:1284–1305.

Schreiner CE, Sutter ML (1992) Topography of excitatory bandwidth in cat primary auditory cortex: single-neuron versus multiple-neuron recordings. J Neurophysiol 68:1487–1502.

Sherman SM, Guillery RW (1998) On the actions that one nerve cell can have on another: distinguishing "drivers" from "modulators. " Proc Natl Acad Sci USA 95:7121–7126.

Steriade M, Llinás R (1988) The functional states of the thalamus and the associated neuronal interplay. Physiol Revs 68:649–742.

Sur M, Esguerra M, Garraghty PE, Kritzer MF, Sherman SM (1987) Morphology of physiologically identified retinogeniculate X- and Y-axons in the cat. J Neurophysiol 58:1–32.

Sutter ML, Schreiner CE, McLean M, O'Connor KN, Loftus WC (1999) Organization of inhibitory frequency receptive fields in cat primary auditory cortex. J Neurophysiol 82:2358–2371.

Treisman A (1999) Solutions to the binding problem: progress through controversy and convergence. Neuron 24:105–110.

Velenovsky DS, Cetas JS, Price RO, Sinex DG, McMullen NT (2003) Functional subregions in primary auditory cortex defined by thalamocortical terminal arbors: an electrophysiological and anterograde labeling study. J Neurosci 23:308–316.

Wall JT (1988) Variable organization in cortical maps of the skin as an indication of the lifelong adaptive capacities of circuits in the mammalian brain. Trends Neurosci 11:549–557.

Weinberg RJ (1997) Are topographic maps fundamental to sensory processing? Brain Res Bull 44:113–116.

Weinberger NM (1998) Physiological memory in primary auditory cortex: characteristics and mechanisms. Neurobiol Learn Mem 70:226–251.

Wilson MA, Molliver ME (1991) The organization of serotonergic projections to cerebral cortex in primates: retrograde transport studies. Neuroscience 44:555–570.

Winer JA (1984) Anatomy of layer IV in cat primary auditory cortex (AI). J Comp Neurol 224:535–567.

Winer JA (1992) The functional architecture of the medial geniculate body and the primary auditory cortex. In: Springer handbook of auditory research, Vol. 1: the mammalian auditory pathway: neuroanatomy (Webster DB, Popper AN, Fay RR, eds), pp 222–409. New York: Springer-Verlag.

Winer JA, Diamond IT, Raczkowski D (1977) Subdivisions of the auditory cortex of the cat: the retrograde transport of horseradish peroxidase to the medial geniculate body and posterior thalamic nuclei. J Comp Neurol 176:387–418.

Winer JA, Larue DT (1987) Patterns of reciprocity in auditory thalamocortical and corticothalamic connections: study with horseradish peroxidase and autoradiographic methods in the rat medial geniculate body. J Comp Neurol 257:282–315.

Winer JA, Lee CC, Imaizumi K, Schreiner CE (2004) Challenges to a neuroanatomical theory of forebrain auditory plasticity. In: Plasticity and signal representation in the auditory system (Merzenich MM, eds), pp 91–106. New York: Klüver Academic/Plenum Publishers.

Winer JA, Morest DK (1983) The neuronal architecture of the dorsal division of the medial geniculate body of the cat: a study with the rapid Golgi method. J Comp Neurol 221:1–30.

(Accepted 29 June 2004)
(Available online 22 September 2004)